Non-collinear magnetic structures of Fe-based amorphous alloys

1991 J. Phys.: Condens. Matter 3 9521

(http://iopscience.iop.org/0953-8984/3/47/024)

J. Phys.: Condens. Matter 3 (1991) 9521–9537. Printed in the UK

Non-collinear magnetic structures of Fe-based amorphous alloys

R A Cowley†, C Patterson‡, N Cowlam§, P K Ivison§, J Martinez‖ and L D Cussen‖

† Department of Physics, University of Oxford, Clarendon Laboratory, Parks Road, Oxford, UK

‡ Department of Physics, University of Edinburgh, Mayfield Road, Edinburgh, UK

§ Department of Physics, University of Sheffield, Sheffield, UK

‖ Institut Laue–Langevin, BP 156 X, 38042 Grenoble, France

Received 15 May 1991, in final form 18 September 1991

Abstract. Neutron scattering techniques have been used to study the structure of amorphous materials. The experiment used both polarized incident and scattered neutron beams and so did not need to assume a collinear magnetic structure. Five different Fe-based amorphous materials were studied and the structures were found to differ. In the case of $Fe_{83}B_{17}$ the spins are canted in a magnetic field of 2 T about 30° from the applied direction. The transverse components have only very short-range order. Other materials show less canting. Fe–Ni amorphous materials shows a large amount of disorder in the spin directions and in the aligned moment. This suggests that the Ni atoms do carry a magnetic moment but that it may be largely misaligned to the Fe moment. Inelastic measurements of the density of magnetic states show a very different distribution to that expected from a powdered ferromagnet. This may arise from 'hidden' short-wavelength excitations.

1. Introduction

The magnetic structure of amorphous materials raises a number of interesting problems of both a theoretical and experimental nature. On the theoretical side the exchange interaction between the ions is probably of Heisenberg character between near neighbours and may well favour a collinear ferromagnetic structure. The ions in an amorphous material are necessarily subject to a local anisotropy arising from their local environment. This randomly directed anisotropy will, in principle, always destroy long-range order (Imry and Ma 1975) and lead to the so-called correlated spin glass state (Chudnovsky *et al* 1986, Chudnovsky 1988). In the presence of a magnetic field, this randomly aligned state becomes a ferromagnetic state with some transverse moment disorder—known as a ferromagnet with wandering axes. The occurrence of non-collinear states in rare earth–iron amorphous materials, such as $TbFe_2$, is well established (Rhyne 1985) and arises from the crystal field effects on the rare earth iron.

Non-collinear structures also arise, as in most spin glasses, if the exchange interactions have both ferromagnetic and antiferromagnetic signs, as discussed for amorphous materials by Parker and Saslow (1988). These effects may arise in amorphous materials because the distances between nearest neighbours vary and the exchange

0953-8984/91/479521 + 17 $03.50

interaction will then also vary and may in some circumstances change sign. The non-collinear structures of Fe–Zr amorphous alloys (Rhyne *et al* 1988) may result from competing exchange interactions.

In contrast, the Fe metalloid (P, B, Si) systems have usually been assumed to have a collinear ferromagnetic structure. This as because the spontaneous ferromagnetic moment was measured to be about $1.8\mu_B$ per Fe atom, which is similar to that found in crystalline BCC iron, and indeed very many of the properties have been very successfully interpreted on this bases. Recently there have been suggestions that the structures might be more complex. Bucholtz *et al* (1986) suggested from magnetostriction measurements that the moments can be randomly aligned, and Melamud *et al* (1987) interpreted Mössbauer results in terms of a spread of moment directions.

In principle, the distribution of the magnetic moment directions can be determined directly by neutron scattering techniques. The experiments are, however, made difficult by the need to separate the nuclear scattering from magnetic scattering, because both are very similar in intensity. In principle, this separation can be achieved by the use of spin-polarized neutron scattering techniques. Since these techniques are very inefficient with neutrons, all previous neutron scattering measurements have used either a polarized incident beam and unpolarized scattered beam or an unpolarized incident beam and analysed the polarization of only the scattered beam. In these experiments, only the magnetic scattering from the ferromagnetically *aligned* moments can be separated from the nuclear scattering and any scattering from *transverse* components of the magnetic moments would not have been distinguished.

The development of the triple-axis spectrometer, IN20, at the Institute Laue Langevin has allowed us to perform measurements with spin-polarized incident and scattered beams which, as described in section 2, enable a direct measurement of the transverse component in some of the Fe-based amorphous alloys. The extent of the transverse canting is different in different samples, and we discuss the possible origins of these differences. The results of a preliminary measurement on one sample, $Fe_{83}B_{17}$, have already been reported (Cowley *et al* 1988). The work on this sample has been repeated and the corrections for the lack of perfect polarization of the incident and scattered beams have been performed more accurately with the consequence that the results reported below are qualitatively, but not quantitatively, the same as those reported earlier.

The Fe_xNi_{1-x} metalloid amorphous alloys have a magnetization which decreases almost linearly with decreasing x (Mizoguchi 1978) for $x > 0.25$. This suggests that the Fe atoms have a magnetic moment of about $1.8\mu_B$ while the Ni atoms have no magnetic moment. For smaller values of x, the average moment and T_c decrease more rapidly and there is evidence of spin glass behaviour (Park *et al* 1986). This can be associated with the difficulty of producing a percolating structure in these dilute systems if there is no moment on the Ni atoms. Measurements have been performed on four of these Fe_xNi_{1-x} alloys with $x = 0.125$, 0.25, 0.5 and 0.75. The results are surprising in that they show a very large amount of disorder in the magnetic structure, and large random transverse moments. This necessarily suggests that the model with no magnetic moment on the Ni atoms is incorrect.

Finally we have studied the magnetic excitations in the $Fe_{83}B_{17}$ sample. This was chosen because the spin-wave parameters, D, deduced from neutron scattering measurements at low wavevectors is a factor of two larger than that deduced from the temperature dependence of the magnetization (Fernandez-Baca *et al* 1987). There is therefore a problem to find the 'hidden excitations'. Secondly, the magnetic excitations near the

maximum of the structure factor have only been studied before using either a spin-polarized incident and unpolarized scattered beam or vice versa (Mook and Tsuei 1977, Shirane *et al* 1982, Paul *et al* 1982, Mook and Lynn 1984) and these measurements do not directly measure the density of excitations (Paul *et al* 1982). Using two spin-polarized beams, a direct measure of the density of states can be made and the results are significantly different from those reported before.

The layout of the paper is as follows. In the next section, the samples, the experimental techniques, and the theory of polarized neutron scattering are described. The third section describes the experimental measurement of the elastic and inelastic scattering cross sections. These are analysed to obtain information about the magnetic structure and excitations in section 4. The results are discussed in the light of current theories in the final section.

2. Experiment

2.1. The samples

The materials were produced as ribbons and wound on a former to produce a sample 35 mm high and 20 mm wide. Cd masks were then placed so that the neutron beam could not scatter from the former or its supports. The samples were wound so that the bulk of the ribbon was vertical along the magnetic field direction.

The majority of the ribbon samples were 50 μm thick and about 1 mm wide and were produced by melt spinning at the University of Sheffield. The other wide-strip samples were commercially produced. Sample A had a composition of $Fe_{83}B_{17}$ while sample B had a composition of $Fe_{78}B_{12}Si_{10}$. Both of these samples were made from ^{11}B to reduce the absorption of the neutron beam. Three samples of commercially available material were used containing natural boron; of these, sample C was a wide 20 mm ribbon of $Fe_{76}B_{12}Si_{12}$ known as Vac 7505. This was studied both with the normal sample holder and with one lengthened to 90 mm so that the bent ends of the ribbon were further removed from the neutron beam. Sample D was made from METGLAS 2605 S2 wide ribbon, $Fe_{78}B_{13}Si_9$. It was studied both in the as-quenched state and then annealed at 500 °C for 900 seconds and re-examined. Sample E was made from a planar cast $Fe_{75}B_{15}Si_{10}$ which was brittle, so the foils were stacked and held in the beam by a holder with Al foil windows.

The Fe–Ni-based alloys were produced at the University of Sheffield by the melt-spinning technique and have the compositions $(Fe_xNi_{1-x})_{78}B_{12}Si_{10}$, with $x = 0.5$, 0.25 and 0.125. These were supplemented by a commercial ribbon VAC 4040 $(Fe_{50}Ni_{50})_{78}B_{10}Si_{10}Mo_2$ and also an intermediate sample with $x = 0.75$ and 1% molybdenum.

2.2. Neutron scattering

The experiments were performed using the triple-axis spectrometer, IN20, at the Institut Laue–Langevin. The spectrometer was used with Heusler alloy crystals as monochromator and analyser, reflecting spin-polarized neutron beams. The horizontal collimation from reactor to detector was 0.5, 1.0, 1.0, 1.0° respectively and the vertical collimation was determined by the height of the crystals and samples and the distances involved. The incident neutron beam had a wavevector of 4.1 $Å^{-1}$, when the

energy width at the elastic position was 3.2 meV (FWHM). The inelastic scattering was studied by varying the scattered neutron energy. A graphite filter was inserted in the incident beam to suppress higher order contaminant neutrons.

The polarization of the neutron beams could be controlled by spin flippers between the monochromator and sample, and between the sample and analyser. The samples were attached to a variable temperature (±1 K) insert in a cryomagnet whose maximum magnetic field was 4 T. The currents in the two parts of the magnet solenoid were slightly different so as to avoid regions of zero field on the neutron beam paths. Care was taken both to ensure that the neutron beam retained its polarization on entering and leaving the cryomagnet and flippers, and to mask the beam so that only the amorphous material was in the incident beam. Unfortunately, when the incident beam flipper was in use, the maximum magnetic field which could be applied to the cryomagnet was 2 T, because the higher stray fields at large fields made it impossible to get a high flipper efficiency given the available coils and power supplies.

In any neutron scattering experiment which depends on the polarization of the beams, the efficiency of the polarizing elements is of crucial importance. The slipping ratio was therefore frequently monitored in the direct beam, both with and without the samples in the beam. As described in the next section, these measurements enabled the polarizing efficiency of the spectrometer and flippers to be obtained.

The magnetic structure of the samples was studied with the spectrometer set for elastic neutron scattering by scanning the wavevector transfer between 1 and 6.6 $Å^{-1}$, with a counting time of about 6 minutes per flipper channel. The inelastic scattering was measured with constant-energy scans with the neutron energy gains of 5, 7 and 10 meV over the same range of wavevector. These scans were made at 250 K and 10 K, and the difference between them gives the magnon scattering at 250 K. At 10 K, there should be negligible magnon scattering in neutron energy gain, and since the elastic scattering is not appreciably temperature dependent, the background is expected to be largely independent of temperature.

In all of the scans the sample was held fixed with the plane of the sample at about 60° to the incident beam. The edges of the former then reduced the scattering at large scattering angles, but this effect is not significant for wavevector transfers less than 5 $Å^{-1}$.

2.3. *Theory of spin-polarized scattering*

The spin-polarized neutron scattering cross sections have been discussed by Moon *et al* (1969) and by Lovesey (1984). The scattering amplitude of a particular atom, ℓ, at $\boldsymbol{R}_{(\ell)}$, can be written in terms of the neutron spin operator, $\boldsymbol{\sigma}$, as

$$V(\ell tt') = \langle t' \,|\, \beta(\ell) + \boldsymbol{\alpha}(\ell)\boldsymbol{\sigma} \,|\, t \rangle \tag{2.1}$$

where the initial neutron spin state is labelled by t and the scattered neutron spin state by t'. $\beta(\ell)$ is the nuclear scattering amplitude averaged over the different nuclear-spin neutron-spin orientations which, for a nucleus of spin. i, is given by

$$\beta = ((i+1)b^+ + ib^-)/(2i+1)$$

while $\alpha(\ell)$ is the sum of the spin-dependent part of the nuclear interaction and the magnetic interaction

$$\boldsymbol{\alpha}(\ell) = (b^+ + b^-)\boldsymbol{i}(\ell)/(2i+1) + d(\ell)\boldsymbol{S}_\perp(\ell)$$

where $d(\ell) = -(\gamma e^2/2mc^2)g_\ell f_\ell(\boldsymbol{Q})$ with $f_\ell(\boldsymbol{Q})$ the magnetic form factor, which is also

assumed to incorporate any orbital contribution, and $\boldsymbol{S}_\perp(\ell)$ is the part of the spin transverse to the wavevector transfer, $\boldsymbol{Q}$. Table 1 shows the nuclear coherent and spin-incoherent cross sections for the elements in the samples (Sears 1984). With the possible exception of ^{10}B, the spin-incoherent cross section is negligible, or occurs only in those isotopes whose natural abundance is very small. Consequently, we can approximate

$$\boldsymbol{\alpha}(\ell) = d(\ell)\boldsymbol{S}_\perp(\ell). \tag{2.2}$$

In the experiments, the magnetic field was applied vertically (the z direction), so the neutron spins t, t' are aligned parallel, $+$, or antiparallel, $-$, to this applied field. If the y axis is chosen along $\boldsymbol{Q}$, then $\boldsymbol{S}_\perp(\boldsymbol{Q})$ is given by $(S_x(\ell), 0, S_z(\ell))$. The expressions for $V(\ell tt')$ can then be calculated as

$$\begin{aligned} V(\ell ++) &= \beta(\ell) + \tfrac{1}{2}d(\ell)S_z(\ell) & V(\ell --) &= \beta(\ell) - \tfrac{1}{2}d(\ell)S_z(\ell) \\ V(\ell +-) &= \tfrac{1}{2}d(\ell)S_x(\ell) & V(\ell -+) &= \tfrac{1}{2}d(\ell)S_x(\ell). \end{aligned} \tag{2.3}$$

The elastic-scattering cross sections are then given by

$$\Sigma^{++} = \mathrm{d}\sigma(++)/\mathrm{d}\Omega = \left|\left\langle \sum_\ell V(\ell ++)\exp(\mathrm{i}\boldsymbol{Q}\cdot\boldsymbol{R}(\ell))\right\rangle\right|^2 \tag{2.4}$$

with analogous expressions for Σ^{--} etc.

These results show that the non-spin flip, Σ^{++} and Σ^{--}, elastic cross sections are dependent upon the nuclear scattering amplitude and the z component of the spin, $\langle S_z(\ell)\rangle$, whereas the spin-flip, Σ^{+-} and Σ^{-+}, elastic scatterings are both equivalent and are a direct measure of $\langle S_x(\ell)\rangle$, the component of the spin operator perpendicular to the applied field and to the wavevector transfer, $\boldsymbol{Q}$.

The inelastic scattering cross sections are given by the same type of analysis but are more complex. If the incident neutron beam has wavevector $\boldsymbol{k}_0$ and the scattered neutron beam, $\boldsymbol{k}$, then

$$\mathrm{d}^2\sigma(tt')/\mathrm{d}\Omega\,\mathrm{d}E = (k/k_0)J(tt', \boldsymbol{Q}, \omega) \tag{2.5}$$

where the frequency, ω, is the frequency transfer in the experiment. If the sample changes from an initial state, m (energy E_m), to a final state, n (energy E_n), then the correlation function is given by

$$J(tt', \boldsymbol{Q}, \omega) = \sum_{n,m} p_m \left|\left\langle n\left|\sum_\ell V(\ell, tt')\exp(\mathrm{i}\boldsymbol{Q}\cdot\boldsymbol{R}(\ell))\right|m\right\rangle\right|^2 \delta(\hbar\omega + E_m - E_n) \tag{2.6}$$

since

$$V(\ell +-) = V(\ell -+) = \tfrac{1}{4}d(\ell)(S^+(\ell) + S^-(\ell)) \tag{2.7}$$

and $J(+-, \boldsymbol{Q}, \omega) = J(-+, \boldsymbol{Q}, \omega)$, and in a system with Heisenberg-like interactions both are sums of $\langle S^+S^-\rangle$ and $\langle S^-S^+\rangle$ correlation functions. This is different from the partially spin-polarized experiments performed earlier (Mook and Tsuei 1977, Paul *et al* 1982, Shirane *et al* 1982) which gave only the *difference* between the $\langle S^+S^-\rangle$ and $\langle S^-S^+\rangle$ correlation functions.

2.4. Correction for depolarization

Unfortunately, Heusler crystals do not reflect only one polarization of the beam and the flippers on IN20 are not perfect. It is therefore necessary to correct the observed

intensities (I^{++}, I^{--}, I^{+-} and I^{-+}) for these effects to obtain reliable estimates of the cross sections, Σ^{++}, Σ^{--} etc. The scattering process can be divided into two parts; some cause depolarization of the beam before the scattering by the sample and this will produce a fraction of the beam of the 'wrong' polarization of magnitude p_1. Other factors cause a fraction of the beam, p_2, having the 'wrong' polarization, to be detected after the scattering. These values, p_1 and p_2, are defined when the flippers are turned off. For example, p_1 results from: incomplete polarization produced by the monochromator; depolarization in the monochromator to sample collimator; depolarization on entry to the cryomagnet; or depolarization in the sample before the scattering process. The efficiencies of the two spin flippers are p_3 in the incident beam and p_4 in the scattered beam.

The observed intensities, I^{++}, can then be related to the cross sections, Σ^{++}, if the ps are small by

$$I^{++} = (1-p_1)(1-p_2)\Sigma^{++} + (1-p_1)p_2\Sigma^{+-} + (1-p_2)p_1\Sigma^{-+} + p_1p_2\Sigma^{--} \tag{2.8}$$

$$I^{--} = (1-p_1-p_3)(1-p_2-p_4)\Sigma^{--} + (1-p_1-p_3)(p_2+p_4)\Sigma^{-+} + (p_1+p_3)(1-p_2-p_4)\Sigma^{+-} + (p_1+p_3)(p_2+p_4)\Sigma^{++} \tag{2.9}$$

$$I^{+-} = (1-p_1)(1-p_2-p_4)\Sigma^{+-} + (1-p_1)(p_2+p_4)\Sigma^{++} + p_1(1-p_2-p_4)\Sigma^{--} + p_1(p_2+p_4)\Sigma^{-+} \tag{2.10}$$

$$I^{-+} = (1-p_1-p_3)(1-p_2)\Sigma^{-+} + (1-p_1-p_3)p_2\Sigma^{--} + (p_1+p_3)(1-p_2)\Sigma^{++} + (p_1+p_3)p_2\Sigma^{+-}. \tag{2.11}$$

Measurements were made of the flipping ratios in the straight-through beam when the different samples were in place and also in the absence of the sample. The results varied with the sample, and also slightly from one measurment to another. The results were, however, consistent with flipper depolarizations; $p_3 = 0.035 \pm 0.01$ and $p_4 = 0.02 \pm 0.01$. The depolarizations, p_1 and p_2, were identical (within the accuracy) and for the machine without a sample; $p_1 = p_2 = 0.027 \pm 0.005$ and somewhat larger for some of the samples are described below, presumably due to depolarization by the samples. The elastic scattering data were analysed by assuming that Σ^{+-} and Σ^{-+} were much smaller than Σ^{++} and Σ^{--}. Using I^{++} divided by $(1-p_1)(1-p_2)$ as an approximation to Σ^{++}, and an analogous expression for Σ^{--}, equations (2.10) and (2.11) were then solved for Σ^{+-} and Σ^{-+}. These results were then used with (2.8) and (2.9) to obtain Σ^{++} and Σ^{--}.

3. Experimental results

3.1. Fe-based amorphous materials

Three samples, A, B and C (described in table 1), wound on the larger former were studied at a temperature of 10 K and in a magnetic field of 2 T with full polarization analysis. The polarization of the beam transmitted through the samples was measured, and in each case there was some depolarization. The results suggested that: for sample A, $p_1 \simeq p_2 = 0.055 \pm 0.005$; for sample B, $p_1 \simeq p_2 = 0.053 \pm 0.005$; and for sample C, $p_1 = p_2 = 0.0375 \pm 0.005$. The results for Σ^{++}, Σ^{--}, Σ^{+-} and Σ^{-+} were then obtained by using the analysis described in the previous section. One test of the success of the

Table 1. Scattering lengths of the isotopes.

Isotope	Abundance	b_{coh} (10^{-14} m)	b_{inc} (10^{-14} m)
^{54}Fe	0.058	0.42	0
^{56}Fe	0.917	1.003	0
^{57}Fe	0.022	0.23	0.2
^{58}Fe	0.003	1.5	0
^{59}Co	1.000	0.25	0.62
^{58}Ni	0.6827	1.44	0
^{60}Ni	0.261	0.28	0
^{61}Ni	0.0113	0.76	0.40
^{62}Ni	0.0359	−0.87	0
^{64}Ni	0.0091	−0.38	0
^{10}B	0.20	−0.01	0.47
^{11}B	0.80	0.66	0.13
^{28}Si	0.92	0.41	0
^{29}Si	0.47	0.47	0.11
^{30}Si	0.31	0.46	0
Mo (Natural)	1.00	0.695	0.015

procedure is the ratio of Σ^{+-}/Σ^{-+} which, in theory, should be 1. Sample A gave 1.02, B gave 1.14 and C gave 0.98 on average, and since these can all be brought to 1 by changing p_1 and p_2 by less than 0.002, the results are very satisfactory. Σ^{+-} and Σ^{-+} have large errors for wavevectors near 3.1 Å^{-1} because Σ^{++} and Σ^{--} are large in this region. The observed intensities, I^{+-} and I^{-+}, for sample A show a peak for $Q = 3.1$ Å^{-1} which is five times background. This is, within error, wholly removed for all of the samples, again suggesting that the data analysis is satisfactory.

The data have been normalized by comparison with the results of Guoan *et al* (1982). In their measurements of sample A, the ratio of $(\Sigma^{--} + \Sigma^{-+})/(\Sigma^{++} + \Sigma^{+-})$ at the maximum was 3.03, whereas in our experiments the ratio is 3.10 ± 0.10—the agreement is similar at other wavevectors. When normalized to $0.83\, b_{Fe}^2 + 0.17\, b_B^2$, the peak of Σ^{--} is 4.7 (Guoan *et al* 1982), and so we have chosen the scale on figure 1 to have the same value for Σ^{--}.

Unfortunately, there are no prior measurements for samples B and C. In the case of sample B, the ratio of the maxima of $(\Sigma^{--} + \Sigma^{-+})/(\Sigma^{++} + \Sigma^{+-})$ is 3.56 ± 0.10, which is different from sample A, but not very different. Consequently we have chosen the scale of figure 2 so that the peak occurs at 4.9. This is equivalent to the sample having nearly the same crystallographic structure as sample A. In a similar manner for sample C (see figure 3), the peak of Σ^{--} was chosen to be 4.9.

Because the data collection for full polarization studies is very slow, and because the equipment required was not available for the whole experiment, the other samples were studied in a magnetic field of 4 T and only the I^{++} and I^{+-} intensities were measured. These results were then analysed by first taking the ratio of Σ^{--}/Σ^{++} for samples A, B and C as a function of wavevector transfer. This ratio was fairly similar for all these samples. The averages of these ratios were used to deduce Σ^{--} from the measured I^{++}. The results for Σ^{++} and Σ^{+-} are then shown in figure 4 (for both before and after the annealing) for sample D. There is clearly very little difference between the results. The scale was chosen by adjusting the peak in Σ^{--} to be the average for samples B and C.

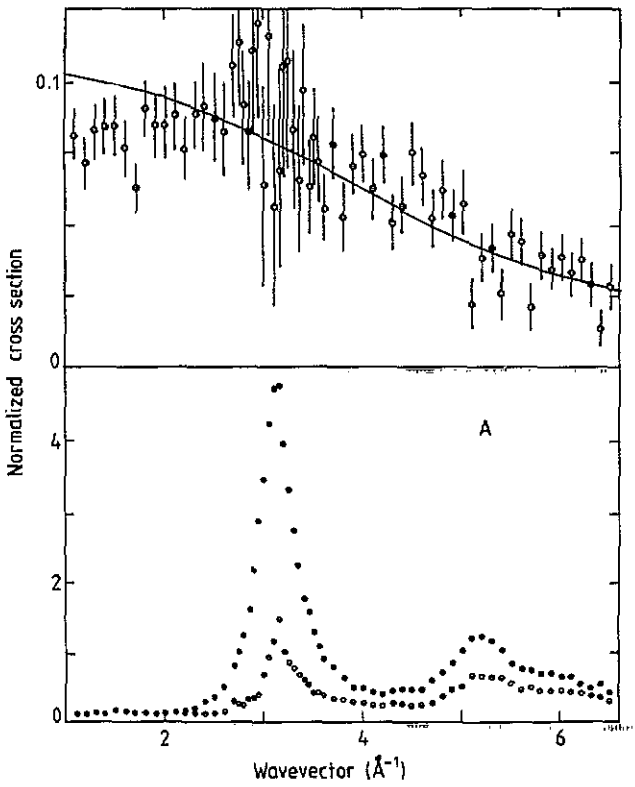

Figure 1. The cross sections, Σ^{++}, ●, Σ^{--}, ○, and in the upper part $(\Sigma^{+-} + \Sigma^{-+})/2$, for A ($Fe_{83}B_{17}$) at 10 K and in a field of 2 T as a function of wavevector (Å^{-1}).

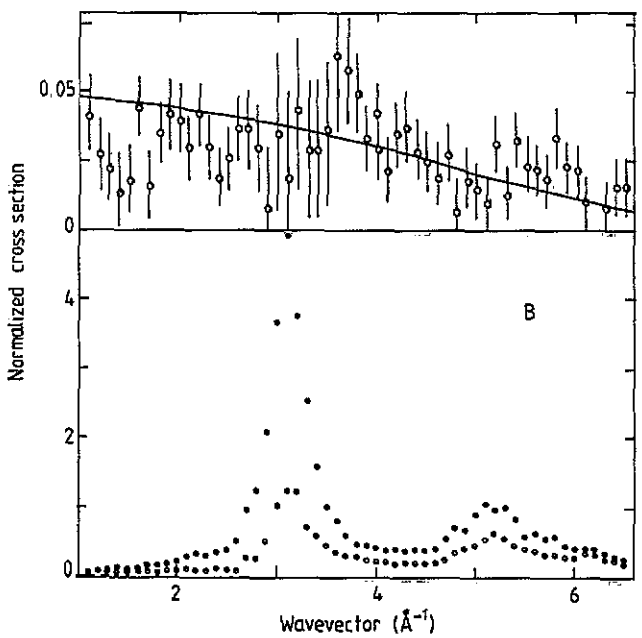

Figure 2. The cross sections, Σ^{++}, ●, Σ^{--}, ○, and in the upper part $(\Sigma^{+-} + \Sigma^{-+})/2$, for B($Fe_{78}B_{12}Si_{10}$) at 10 K and in a field of 2 T.

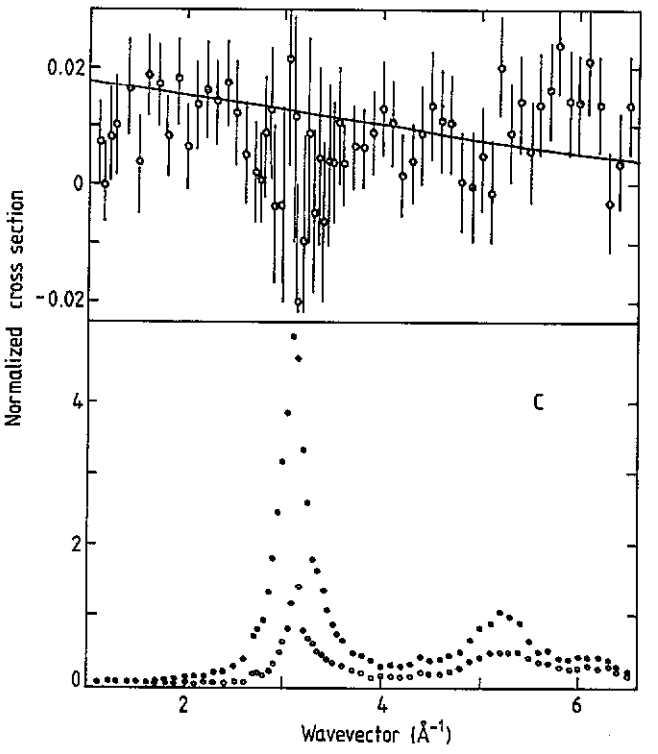

Figure 3. The cross sections, Σ^{++}, ●, Σ^{--}, ○, and in the upper part $(\Sigma^{+-} + \Sigma^{-+})/2$, for C ($Fe_{76}B_{12}Si_{12}$) at 10 K and in a field of 2 T.

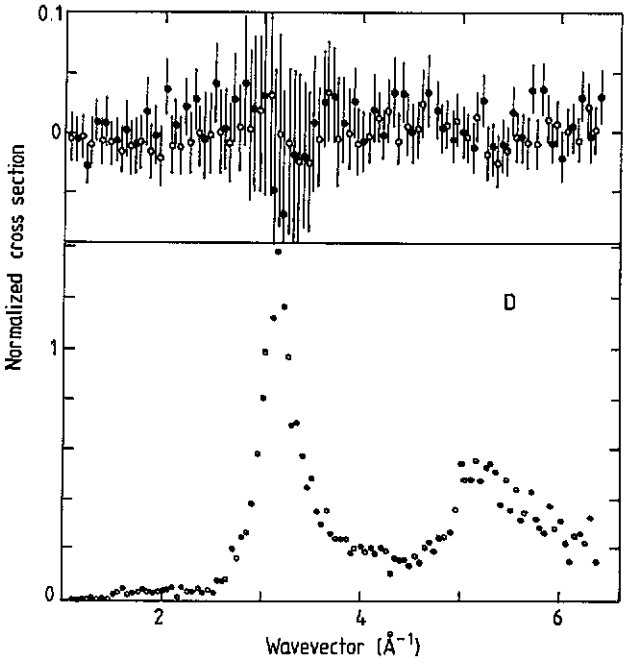

Figure 4. The cross section, Σ^{--}, lower, and Σ^{-+}, upper, for annealed, ●, and as-received sample D, ○, at 10 K and in a field of 4 T.

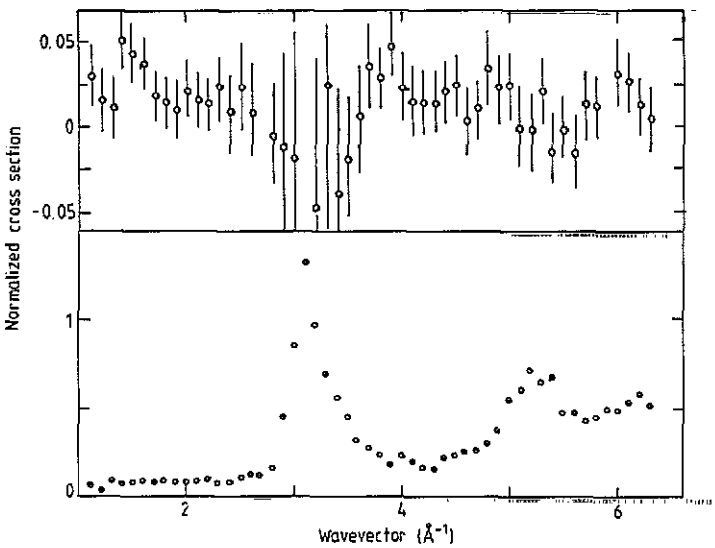

Figure 5. The cross sections, Σ^{--}, lower, and Σ^{-+}, upper, for sample E (planar cast $Fe_{75}B_{15}Si_{10}$) at 10 K and in a field of 4 T.

A similar procedure was adopted for sample E—the planar cast $Fe_{75}B_{15}Si_{10}$—and the results are shown in figure 5.

3.2. Fe–Ni-based alloys

All of these samples were studied at 10 K and in a magnetic field of 4 T by measuring I^{++} and I^{+-}. Because the ferromagnetic moment decreases steadily with increasing Ni concentration, it is to be expected that the difference between Σ^{++} and Σ^{--} decreases as the Ni concentration increases. Consequently the sample with $x = 0.125$ (Fe_xNi_{1-x}) was analysed by assuming that $\Sigma^{++} = \Sigma^{--}$. Measurements of the straight-through beam gave negligible depolarization produced by the sample for $x < 0.75$; in the case of $x = 0.75$, $p_1 = p_2 = 0.030 \pm 0.005$. The results for $x = 0.125$ are shown in figure 6—since there is no significant peak in Σ^{+-} for $Q = 3.1$ Å^{-1}, it was concluded that the analysis gave reasonable results. The technique was then applied to the results for $x = 0.25$ and figure 6 shows that the results are also very reasonable. Figure 7 shows similar results obtained for $x = 0.5$. In this case there is an increase in Σ^{+-} for wavevectors near $Q = 3.1$ Å^{-1}, but it is not so significant as to be certain.

For $x = 0.75$, the results were different. If it was assumed that $I^{++} = I^{--}$, then a large peak in Σ^{+-} was present for $Q \approx 3.1$ Å^{-1}. Similarly, if it was assumed that the ratio of I^{++}/I^{--} was the same as for samples B and C of the Fe-based alloys, then the resulting Σ^{+-} was strongly negative in this region. We have therefore chosen the ratio I^{++}/I^{--} so that there is no substantial peak or dip in Σ^{+-} for $Q = 3.1$ Å^{-1}. This is because none of the other samples showed such a peak and the ratio is relatively sensitive to this ratio in a narrow range of Q. The results shown in figure 7 were obtained with the difference between I^{++} and I^{--} one half the amount it was for samples B and C of the Fe-based alloys.

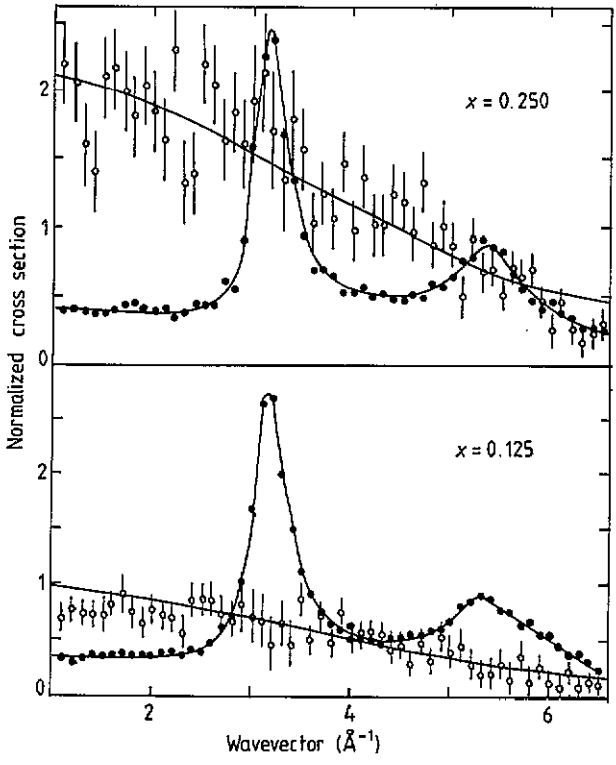

Figure 6. The cross sections, Σ^{--}, ●, and 10 Σ^{+-}, ○, for Fe_x–Ni_{1-x} amorphous alloys with $x = 0.125$ (lower) and $x = 0.25$ (upper) at 10 K and in a field of 4 T as a function of wavevector (Å^{-1}).

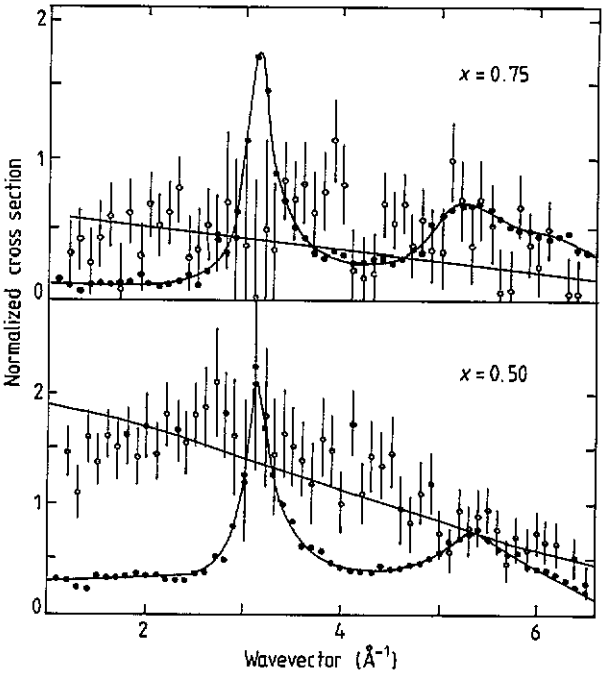

Figure 7. The cross sections, Σ^{--}, ●, and 10 Σ^{-+}, ○, for Fe_x–Ni_{1-x} amorphous alloys with $x = 0.5$ (lower) and $x = 0.75$ (upper) at 10 K and in a field of 4 T.

The normalization of the intensities was performed by assuming that the peak in the Σ^{++} cross section was proportional to

$$D = \left| \sum_i c_i b_i^{\mu} \right|^2 \Big/ \sum_i c_i b_i^2$$

where the summation is over each nuclear species, and b_i^{μ} is the appropriate coherent scattering cross section, b_i, except for Fe, for which it is the difference between the nuclear and magnetic cross sections. This approximation assumes that there is no ferromagnetic moment on the Ni ions, that the structure of the different alloys is the same, and that, for $Q = 3.1$ Å^{-1}, the scattering is fully in phase. In view of all these approximations, the normalization procedure is necessarily approximate but is unlikely to be in error by more than 20%, and the main results of the canting are largely dependent on the small wavevector-transfer part of the spectrum for which the substraction is relatively unimportant.

3.3. Inelastic scattering

The spin-polarized inelastic scattering was studied in detail in one Fe-based sample, A, and in only one of the Fe–Ni samples—the one with 25% of Fe. It was found that, away from the elastic scattering, all of the intensities were very similar—I^{++}, I^{--}, and I^{+-} were never different by more than a factor of two. The intensities were also weak, being about 1½ counts/minute at 10 K and 3 counts min^{-1} at 250 K. At these low counting levels the background is very important and the experiments very lengthy, so the experiment concentrated on measuring the I^{+-} and I^{-+} intensities. Since the inelastic excitation scattering is expected to be proportional to the Bose–Einstein factor, the scattering from the excitations was obtained as the difference between I^{+-} and I^{-+} as measured at 250 K and at 10 K. The elastic scattering and the background is very similar at both temperatures. No corrections were made for the depolarization of the instrument or the sample because I^{++} and I^{--} were of comparable size to I^{+-} and I^{-+}.

The experiments were performed as constant energy scans with the wavevector transfer varied between 1 and 6.5 Å^{-1}. Results were obtained for the Fe-based sample with the energy held at neutron energy gains of 5, 7 and 10 meV—the results are shown in figure 8. They suggest that there is a broad peak in the intensity centred around a wavevector transfer of 4 Å^{-1} with a width of at least 4 Å^{-1}. The intensity of the scattering increases with decreasing energy transfer by an amount that is only slightly less than the $1/\omega$ dependence expected if there was a constant density of states for the excitations.

Less detailed measurements were made of the $Fe_{0.25}$ $Ni_{0.75}$ samples, and figure 9 shows the result for a scan with an energy transfer of 5 meV. The result is qualitatively similar to those shown in figure 8. The peak is, however, centred at a lower wavevector of 3.5 Å^{-1}, has a width of about 3.0 Å^{-1}, and is about double the intensity of the measurements shown in figure 8.

4. Discussion of the results

4.1. Fe-based alloys

The most complete measurements of the elastic scattering are shown for samples A, B and C in figures 1–3. The Σ^{++} and Σ^{--} cross section are similar for all the three different

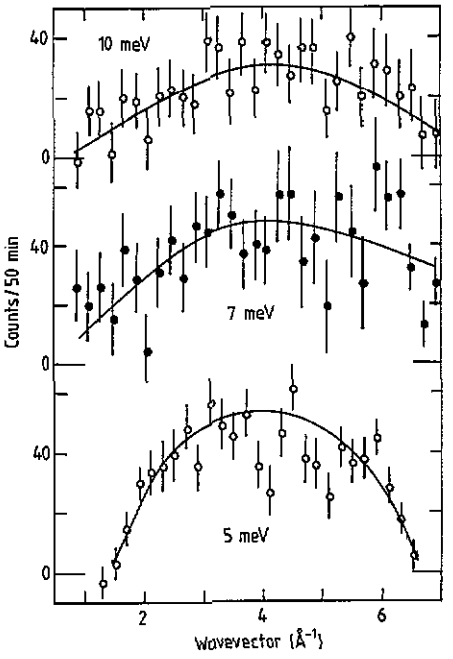

Figure 8. The inelastic scattering, Σ^{-+} (250 K) − Σ^{-+} (10 K), for $Fe_{83}B_{17}$ and energy transfers of 5, 7 and 10 meV as a function of wavevector (Å^{-1}).

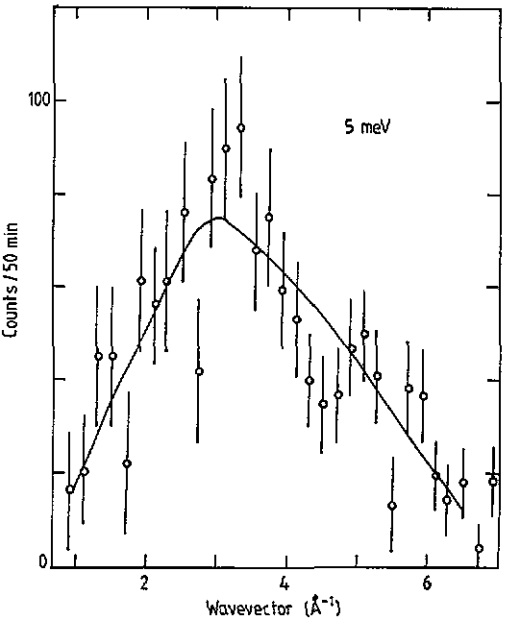

Figure 9. The inelastic scattering, Σ^{-+} (250 K) − Σ^{-+} (10 K) for $Fe_{0.25}Ni_{0.75}$ and an energy transfer of 5 meV.

samples, showing that they have very similar amorphous structures. The spin-flip cross sections, Σ^{+-} and Σ^{-+}, are within error the same for each material, but are different for samples A, B and C. The cross section is largest for sample A and follows a decrease as the wavevector transfer increases. The results are less clear for samples B and C, but the cross section in both cases is certainly smaller and tends to decrease with increasing wavevector. The results cannot be explained as nuclear spin-incoherent scattering firstly because this cross section is too small. For sample A, the nuclear incoherent scattering is calculated (from table 1) to have a cross section of 0.008 barns, an order of magnitude less than the experimental result shown in figure 1, while for samples B and C, the cross section of 0.006, which is also smaller than the results. Secondly, the decrease at large wavevector is more rapid than would be expected from the Debye–Waller factor at 10K. Thirdly, the spin-flip scattering might arise if the samples contained significant amounts of hydrogen (~0.5%). It is unlikely that hydrogen would be present after the argon-arc melting and melt spinning in air, and a detailed analysis of a Cu–Ti alloy produced in the same way showed that the hydrogen was not present in a concentration of more than parts/million. The Fe and Fe/Ni samples would be expected to have even less hydrogen in them. We conclude that the spin-flip scattering arises from magnetic scattering, and in particular from the moments not being fully aligned along the applied magnetic field.

The cross section for the scattering from the transverse magnetic moments is the product of the square of the form factor for the magnetic ions and a correlation function describing the correlation between the transverse moments. The fall-off in the cross section is similar to σ that expected from a magnetic form factor. We have therefore

compared the results with the form factor of iron as deduced by Lisher and Forsyth (1971)

$$f(Q) = 0.3854\exp(-0.08517\,WQ^2) + 0.6326\exp(-0.03209\,WQ^2) - 0.0173$$

where the parameter W (Bletry and Sadoc 1975) was introduced to account for the broadening of $f(Q)$ in an amorphous sample. Previous measurements (Guoan *et al* 1982) have suggested that $W = 0.8$, corresponding to the magnetization density in the amorphous material having a radius only 90% of that in the crystal.

A comparison of our results for Σ^{+-} (figure 1) with $|f(Q)|^2$ shows that our data extends to larger Q than predicted by the form factor, and the solid surves in figures 1–3 were calculated with $W = 0.35$, corresponding to a magnetization radius of only 60% of that in the crystal. This result is very surprising, but is supported by the results for Σ^{++} and Σ^{--}. For all of the materials, the ratio of Σ^{++} to Σ^{--} is about 0.2 for $Q = 3$ Å^{-1} and 0.7 for $Q = 6$ Å^{-1}. These must therefore be significant magnetic scattering at the larger wavevectors suggesting that the form factor does not decrease nearly as rapidly as found in crystalline Fe.

The comparison of the square of the form factor with the results in figure 1 shows that there are significant discrepancies, particularly at small wavevectors. These presumably arise from correlations between the transverse moments of the spins which we have neglected. It might be reasonable to expect a broad peak near $Q = 3.1$ Å^{-1} to arise from these correlations, but the quality of the data makes it difficult to estimate the correlation volume. Nevertheless the results suggest that the correlation length is probably quite small. We shall therefore discuss the extent of the canting of the spins in terms of a model in which the transverse components of the spins are uncorrelated.

The magnitude of the transverse-spin components can be obtained from the magnetic cross section, and the intensity of the spin-flip scattering. If the transverse moment is μ_x (Bohr magnetons) then, for sample A,

$$\Sigma^{+-}(Q = 0) = \langle\mu_x^2\rangle 0.089$$

when normalized to the total nuclear scattering, as in figure 1. The solid line has $\Sigma^{+-}(0) = 0.11$ but this is most likely an over-estimate for the extrapolation $Q \to 0$, and a more reasonable value of 0.09 gives

$$\langle\mu_x^2\rangle = 1.0 \pm 0.2.$$

Since the aligned longitudinal moment is $1.75\mu_B$ (Guoan *et al* 1982), these results suggest that the spin is canted by $30 \pm 6°$. The total average moment, μ, associated with each ion can be obtained by assuming that $\langle\mu_y^2\rangle = \langle\mu_x^2\rangle$ when $\mu = 2.25 \pm 0.1\mu_B$.

Similar calculations can be performed for samples B and C with the results shown in table 2. It is worth noting that the spin-flip scattering decreases as the square of the canting angle, θ, for small angles, so the experiment is quite insensitive to small angles.

Further confirmation that the spins are most canted in sample A lies in the low-wavevector region of the Σ^{++} and Σ^{--} cross sections. If there is appreciable randomness in the direction or length of the spins, then this will give rise to a contribution to Σ^{++} and Σ^{--} at small wavevectors. The scattering in this region is appreciably larger for sample A than for samples B and C.

Sample D was examined both before and after annealing. There is little difference in Σ^{++} and Σ^{--}, and in both cases Σ^{+-} is small, although the results do suggest that the Σ^{+-} may be slightly larger in the annealed than in the unannealed form. Even in the annealed case, the Σ^{+-} scattering is so small that the degree of any canting cannot be

Table 2. Transverse moments and canting angle of Fe-based materials.

Sample	Composition	$\langle\mu_x^2\rangle$ (μ_B^2)	$\langle\theta^2\rangle^{1/2}$ (deg)
A	$Fe_{83}B_{17}$	1 ± 0.2	30 ± 6
B	$Fe_{78}B_{12}Si_{10}$	0.2 ± 0.1	14 ± 15
C	$Fe_{76}B_{12}Si_{12}$ (VAC 7505)	0.45 ± 0.15	21 ± 5
D	$Fe_{78}B_{13}Si_9$ (M2605S2)	0 ± 0.1	0 ± 7
E	$Fe_{75}B_{15}Si_{10}$	0.25 ± 0.2	16 ± 11

Table 3. Moments in Fe_xNi_{1-x}—transverse moments, random longitudinal moments, ordered longitudinal moments and random longitudinal moments if Ni had no moment and Fe the same moment as in the pure Fe-based system.

x	$\langle\mu_x\rangle^2$	$\langle\mu_z^2\rangle_R$	$\langle\mu_z\rangle^2$	$\langle\mu_z^2\rangle_T$
0.125	1.0 ± 0.2	1.9 ± 0.3	0.05	0.33
0.25	2.4 ± 0.3	2.6 ± 0.4	0.19	0.57
0.5	1.7 ± 0.5	1.9 ± 0.5	0.77	0.76
0.75	0.6 ± 0.3	0.45 ± 0.2	1.74	0.57

reliably measured (table 2). Sample E also has only a small amount of canting, as shown in table 2.

In conclusion, our results strongly suggest that there is appreciable canting in some Fe-based amorphous alloys and that the canting varies from sample to sample. The results suggest that the canting is largely uncorrelated from site to site. One surprising features of the results is that the magnetization density seems to be of much smaller radius than that in crystalline Fe.

4.2. Fe–Ni alloys

The results for the Fe–Ni alloys are shown in figures 6 and 7. Qualitatively, the results are similar for Σ^{++} and Σ^{--} to the Fe-based alloys and to one another. In detail, however, the low-Q part of Σ^{++} increases with increasing Ni content. In part, this arises from the different nuclear scattering lengths of the isotopes of Ni and of Fe, but this incoherence can account for only about one third of the intensity for $Q \sim 1$ Å^{-1}. Since the Ni ions on average are assumed to have nearly zero contribution to the spontaneous moment, there is also a fluctuation in the magnitude of the longitudinal magnetic moments. We have calculated this by taking the observed intensity for wavevectors between 1 and 2 Å^{-1} and subtracting the nuclear incoherent scattering to calculate $\langle\mu_z^2\rangle_R$ (the random part of the longitudinal moments), as shown in table 3. The Σ^{+-} cross section is compared with the form factor (with $W = 0.35$) in figures 6 and 7. Clearly Σ^{+-} closely approximates this form for $x = 0.125$ and 0.25, showing that the transverse moments are largely uncorrelated and have a very similar form factor to the Fe-based amorphous alloys. The transverse moments were calculated as for the Fe-based alloys and the result are shown in table 3. The Σ^{+-} cross section was less satisfactorily determined for $x = 0.75$ and 0.5. This is because of the difficulty in knowing the backgrounds, as described in section 3.2.

In the calculations of $\langle\mu_x^2\rangle$, we have taken $\Sigma^{+-}(0) = 0.15 \pm 0.05$ for $x = 0.5$ and 0.05 ± 0.025 for $x = 0.75$.

The results shown in table 3 are unexpected because $\langle\mu_x^2\rangle$ and $\langle\mu_z^2\rangle_R$ are clearly similar for all the alloys and because $\langle\mu_z^2\rangle_R$ is larger than the mean moment squared, $\langle\mu_z\rangle^2$, for $x < 0.6$, and more than $\langle\mu_z^2\rangle_T$, which is the random moment calculated assuming that there was a constant fully aligned moment on each Fe ion and zero moment on each Ni ion. These results can only be understood if there is considerably more disordered moment than is given by this simple picture. Indeed the results for $x = 0.5$ and 0.25 suggest that the moment per site is about $2.6\,\mu_B$, whereas the aligned moment is less than $1\,\mu_B$ and the moment per site is still about $2.0\,\mu_B$ even when $x = 0.125$. These results suggest that the Ni ions do have a moment which is nearly comparable to that on the Fe atoms, but that this is randomly oriented and does not contribute to the ordered moment when a magnetic field is applied.

4.3. Inelastic measurements

The inelastic measurements shown in figures 8 and 9 are measures of the density of magnetic excitations. In the case of sample A, it is known (Fernandez-Baca *et al* 1987) that there are long-wavelength well-defined spin waves with $D = 153$ meV Å^{-2}, and we have confirmed this D value directly with our sample. A model of the amorphous material is to treat it as a powdered crystalline material and then to broaden the results by the width of the first peak in the structure factor. In our case this will produce scattering near the peak with $Q = 3.1$ Å^{-1}, with a width in wavevector determined by the D value, $\Delta q = 2(\hbar\omega/D)^{1/2}$. For energy transfers of 5 and 10 meV, this gives $\Delta q = 0.36$ Å^{-1} and 0.51 Å^{-1}, respectively. Even then, broadening with the width of the peak in the structure factor, 0.32 Å^{-1}, fails to account for the large widths shown in figure 8. We conclude that this simple model of the magnetic excitations is inconsistent with our results.

Experiments using only a polarized incident or scattered beam (Mook and Tsuei 1977, Mook and Lynn 1984) have suggested that there is a low energy gap in the density of states of $Q \sim 3.1$ Å^{-1}. These measurements depend on the difference between Σ^+ and Σ^{-+}, and so do not directly measure the density of states (Paul *et al* 1982). In contrast, the measurements reported here directly give the density of states. Since Σ^{+-} decreases with increasing energy roughly as $1/\omega$ for $Q = 3.1$ Å^{-1}, the density of states is almost constant, at least between 5 and 10 meV.

5. Conclusions

The experiment has shown that fully spin-polarized neutron scattering experiments can provide unique information about the stucture and dynamics of amorphous materials. The results show that in Fe-based materials the magnetic moments are sometimes canted by as much as 30°, but in other samples are less canted in fields of 2T. This canting may arise either from the effect of the local crystal field, which in an amorphous material is necessarily randomly directed, or from exchange interactions of different signs. In amorphous materials the distances between neighbours vary, and hence the exchange interactions will vary. In the Fe-based materials this may even cause a change in sign since FCC Fe is known to be antiferromagnetic, unlike BCC Fe. If the canting arises from local crystal fields, this implies that the Fe-based materials are ferromagnetic materials

with a wandering axis, and that by controlling the local fields it may be possible to control the magnetostriction and anisotropy of amorphous materials (Gibbs 1990). Neutron scattering will certainly play an important role in understanding these effects.

In the case of the Fe–Ni alloys the results are even more surprising. They suggest that there is a large random moment and that the moments are randomly directed for x larger than about 0.6. This presumably arises because either the Fe–Ni or Ni–Ni exchange constants are antiferromagnetic, leading to a largely random spin-glass type of structure.

The experiments on the dynamics have for the first time measured the density of magnetic excitations close to the peak of the structure factor. The results show that the density of states has no gap and is almost independent of frequency. The width in wavevector is much larger than expected for a powder model of an amorphous material and the reason for this is unknown.

Unfortunately fully spin-polarized neutron scattering experiments are difficult and time consuming but the uniqueness of the information they provide about amorphous materials ensures that they will continue to be performed hopefully over a larger wavevector range and with a wider variety of samples.

Acknowledgments

We are grateful for the use of the IN20 spectrometer at ILL and for the financial support of the Science and Engineering Research Council.

References

Bletry J and Sadoc J F 1975 *J. Phys. F: Met. Phys.* **5** L111
Bucholtz F, Koo K P, Dandridge A and Sigel G H 1986 *J. Magn. Magn. Mater.* **54–57** 1607
Chudnovsky M, Saslow W M and Serota R A 1986 *Phys. Rev.* B **33** 251
Chudnovsky M 1988 *J. Appl. Phys.* **64** 5770
Cowley R A, Cowlam N and Cussens L D 1988 *J. Physique Coll.* **49** C8 1285
Fernandez-Baca J A, Lynn J W, Rhyne J J and Fish G F 1987 *Phys. Rev.* B **36** 8497
Gibbs M R J 1990 *J. Magn. Magn. Mater.* **83** 329
Guoan Wu, Cowlam N, Davies H A, Cowley R A, Paul D McK and Stirling W G 1982 *J. Physique Coll.* **13** C7 71
Imry Y and Ma S 1975 *Phys. Rev. Lett.* **35** 1399
Lisher E J and Forsyth J B 1971 *Acta Crystallogr.* A **27** 545
Lovesey S W 1984 *Theory of neutron scattering from condensed matter* vol 2 (Oxford: Clarendon)
Melamud M, Swartzendruber L J, Bennett L H, Cullen J and Wun-Fogle M 1987 *J. Appl. Phys.* **61** 3644
Mizoguchi T 1978 *Sci. Rep. RITU* A Suppl. 117
Mook H A and Lynn J W 1984 *Phys. Rev.* B **29** 4056
Mook H A and Tsuei C C 1977 *Phys. Rev.* B **16** 2184
Moon R M, Riste T and Koehler W C 1969 *Phys. Rev.* **181** 920
Park M J, Bhagat S M, Manheimer M A and Moorjani K 1986 *Phys. Rev.* B **33** 2070
Parker G N and Saslow W M 1988 *Phys. Rev.* B **38** 11718
Paul D McK, Cowley R A, Stirling W G, Cowlam N and Davies H A 1982 *J. Phys. F: Met. Phys.* **12** 2687
Rhyne J J 1985 *IEEE Trans. Magn.* **MAG-21** 1990
Rhyne J J, Erwin R W, Fernandez-Baca J A and Fish G E 1988 *J. Appl. Phys.* **63** 4080
Sears 1984 *Thermal Neutron Scattering Lengths* AECL report 8490
Shirane G, Axe J D, Majkrzak C F and Mizoguchi T 1982 *Phys. Rev.* B **26** 2575